Improved Prediction of Oil Recovery From Waterflooded Fractured Reservoirs Using Homogenization

Hamidreza Salimi, SPE, and **Johannes Bruining,** SPE, Delft University of Technology

Summary

Most simulations of waterflooding in fractured media are based on the Warren and Root (WR) approach, which uses an empirical transfer function between the fracture and matrix block. We use homogenization to obtain an improved flow model in fractured media, leading to an integro-differential equation; also called the boundary-condition (BC) approach. We formulate a well-posed numerical 3D model for the BC approach. This paper derives this numerical model to solve full 3D integro-differential equations in a field reservoir simulation. We compare the results of the upscaled model with ECLIPSE™ results. For the interpretation, it is useful to define three dimensionless parameters that characterize the oil production in fractured media. The most important of these parameters is a Peclet number, defined as the ratio between the time required to imbibe water into the matrix block and the travel time of water in the fracture system. The results of the WR approach and the BC approach are in good agreement when the travel time is of the same order of magnitude as the imbibition time. However, if the travel time is shorter or longer than the imbibition time, the approaches give different results. The BC approach allows the use of transfer functions based on fundamental principles (e.g., the use of a rate-dependent capillary pressure function). When implemented, it can be used to improve recovery predictions for waterflooded fractured reservoirs.

Introduction

Naturally fractured petroleum reservoirs represent more than 20% of the world's oil and gas reserves (Saidi 1983), but are among the most complicated class of reservoirs to produce efficiently. Naturally fractured reservoirs (NFRs) comprise an interconnected fracture system that provides the main flow paths and the reservoir rock, or matrix, that acts as the main source of hydrocarbons.

From the geological point of view, it is possible to distinguish between various types of fractured reservoirs (Nelson 1985; Stearns 1969; Stearns 1972). The most important aspect is whether the fracture network provides a continuous flow path (Saidi 1983) or whether it has regions with different fracture geometries or systems consisting of a hierarchy of fracture systems at different scales (multiscale fractures) (Yu-Shu Wu 2004; Gasem et al. 2008). When the fracture network is not continuous, the reservoir can be split up into fractured and non-fractured domains. Also in the fractured domains, the reservoir is heterogeneous, with, for example, different fracture densities, fracture apertures, and anisotropies. In some approximate sense, the fractured reservoirs show some repetition of fractured subdomains. This aspect will be used for obtaining averaged properties of the subdomains. The same idea can also be used as a first guess to obtain the global flow field. Alternatively, it is possible to use the global flow field to obtain BCs at the local scale and repeat this procedure until convergence has been obtained.

Flow modeling in fractured reservoirs was greatly advanced by Barenblatt et al. (1960), who introduced the concept of "dual porosity." In addition, they introduced the transfer function and shape factor. From the geometrical point of view, Barenblatt assumed that the fracture system is regular "to some extent." Warren and Root (1963) used the dual-porosity model and applied it to a well-test analysis. They also introduced the sugar-cube model, which has been the basis of many of the fractured-reservoir simulators since that time. The dual-porosity model of WR for examining pressure drawdown and buildup phenomena in NFRs was extended by Kazemi et al. (1969, 1992) to interpret interference-test results. These ideas were extended with the introduction of the so-called dual-permeability model, in which the matrix blocks can also contribute to the global flow, depending on the ratio of fracture permeability to matrix-block permeability.

The transfer function is semi-empirical. It relates the fluid flow at the interface of matrix and fracture to the driving force (e.g., average phase-pressure difference between fracture and matrix). More recently, the ideas were extended with the derivation of transfer functions based on fundamental transport modeling. Dutra and Aziz (1992) presented a model that takes into account the transient nature of the imbibition process and the effect of variation in fracture saturation. Sarma and Aziz (2006) proposed a general numerical technique to calculate the shape factor for any arbitrary shape of the matrix block (e.g., non-orthogonal fractures).

One drawback is that the transfer-function approach ignores the history-dependent nature of the transfer process. This would be justified only if the time dependence of the BC around the matrix block were weak.

A new approach was introduced by Douglas and Arbogast (1989, 1990, 1991), in which they applied a new upscaling technique (homogenization) to derive the model equations for flow in fractured reservoirs, which does not suffer from the above-mentioned drawback. Full derivations can be found in Arbogast (1993a, 1993b, 1997) and in Arbogast and Lehr (2006). These papers were written for a mathematically oriented audience.

The following brief description of homogenization for fractured media emphasizes the physics. A microscopic transport model in a fractured medium consists of (1) the flow equations in the fracture, (2) the flow equations in the matrix, and (3) the BCs between matrix and fracture (i.e., continuity of capillary pressure unless one of the phases is at residual saturation and continuity of flux). Application of homogenization leads to a transport equation in the fracture system with a source term that describes the amount of oil that is transferred from the matrix blocks to the fracture. Homogenization suggests that for the calculation of the source term we need to solve the two-phase-flow equations in the matrix block subject to a boundary potential that is given by the potential of the fracture system on the macroscale. One of the assumptions used in homogenization is that the order of magnitude of each term in the transport equations can be related to a single scaling parameter (ε). This scaling parameter describes the ratio of the local scale to the global scale. This means that the order of magnitude of all characteristic dimensionless numbers must be expressed in terms of this scaling ratio. The second assumption is that the domain can be subdivided into parts (unit cells) in which the flow equations can be solved using periodic BCs. This implies that a condition for the application of homogenization is that the separation of scales is possible. The main advantage of homogenization is that it allows deriving the exchange rate between matrix and fracture on the basis of first principles. After averaging the equations over the unit cell, we find the upscaled equations. Different upscaled model equations are obtained when different orders of magnitudes

This paper (SPE 115361) was accepted for presentation at the SPE Annual Technical Conference and Exhibition, Denver, 21–24 September 2008, and revised for publication. Original manuscript received for review 26 June 2008. Revised manuscript received for review 19 December 2008. Paper peer approved 21 January 2009.

for the dimensionless parameters are used. This allows the definition of subdomains in the parameter space that give qualitatively different behavior. It is the purpose of this paper to quantify these regimes of different behavior based on a characteristic dimensionless number. For problems of engineering interest, these orders of magnitude can be easily assigned. To illustrate the advantages and disadvantages of the BC approach (homogenization), we compare it with the WR approach using ECLIPSE.

We ignored the time-dependent BCs for the matrix block in a previous paper (Namdar Zanganeh et al. 2007). The present paper shows how to incorporate the time-dependent BCs for the matrix block. It also stresses other aspects (i.e., the definition and importance of characteristic numbers). Moreover, it uses a fully implicit approach to solve the model equations, which now include gravity.

The paper is organized as follows. First, we describe the general framework of homogenization on the basis of a physical model for a fractured reservoir. After that, we introduce the dimensionless numbers. Here, we also define a Peclet number as a ratio between the time of capillary diffusion of oil from the matrix to the fracture and the residence time of water in the reservoir. Subsequently, the results are interpreted in terms of the dimensionless groups. We end with some conclusions. Appendix A shows the derivation of the effective-fracture-permeability tensor. Appendix B gives the full 3D numerical model.

Method of Homogenization

Physical Model. Consider a fracture network with matrix blocks in between. The matrix blocks are completely surrounded by fractures except for some isolated crushed zones with zero permeability holding the matrix blocks together. The local fracture porosity and intrinsic permeability evaluated inside the fracture are denoted by ϕ_f^* and k_f^*, respectively. We define the intrinsic fracture permeability k_f^* on the basis of the fracture aperture. Because the main purpose of this paper is to illustrate only the essential concepts, we assume here that the symmetry of the fracture pattern is such that the fracture permeability can be considered isotropic, but this assumption can be easily relaxed (see Appendix A). The global fracture porosity and effective permeability evaluated with respect to the bulk volume are denoted by ϕ_f and k_f, respectively. The matrix porosity and matrix permeability are denoted by ϕ_m and k_m. Note that small differences between intrinsic and global values of the matrix porosity and permeability are ignored, and only the global values are used here. We consider only two-phase (oil and water) incompressible flow where the water viscosity μ_w and oil viscosity μ_o, are assumed to be constant. We use the two-phase ($\alpha = o, w$) extension of Darcy's law for constant fluid densities:

$$\mathbf{u}_{\alpha f}^* = -\frac{k_f^* k_{r\alpha,f}}{\mu_\alpha}\nabla\left(P_{\alpha f} + \rho_\alpha g z\right) := -\lambda_{\alpha f}^* \nabla\Phi_{\alpha f} \quad \text{and} \quad \mathbf{u}_{\alpha m} = -\frac{k_m k_{r\alpha,m}}{\mu_\alpha}\nabla\Phi_{\alpha m} := -\lambda_{\alpha m}\nabla\Phi_{\alpha m} \quad \ldots\ldots\ldots\ldots (1)$$

In these equations, the superscript (*) denotes the intrinsic fracture properties. Here, z is the vertically upward direction. Note that the fracture permeability and matrix permeability are considered isotropic. Relative permeabilities are denoted by $k_{rw,\zeta}$ and $k_{ro,\zeta}$, where $\zeta = f, m$ indicates the fracture and matrix systems. In the same way, $P_{c\zeta}$ denotes the capillary pressure. There is capillary pressure continuity at the boundary of fractures and matrix blocks unless one of the phases either in the matrix or in the fracture is immobile (Duijn et al. 1995). Indeed, when one of the phases is immobile, the pressure of that phase depends on local conditions and cannot be determined globally. Hence, the capillary pressure, which is the difference between the phase pressure of the nonwetting phase and that of the wetting phase, is not continuous. However, as residual saturations do not flow, this has no relevance for the modeling. Continuity of force, and, hence, continuity of phase pressures, implies continuity of capillary pressure when both phases are mobile.

The disparity of permeability between the fracture and matrix has a consequence that only a small deviation from connate-water saturation in the fracture leads to a water saturation close to $1-S_{or}$ in the part of the matrix adjacent to the fracture.

Homogenization Procedure. The homogenization procedure is divided into four major steps, based on specific assumptions that are stated in each step.

The first step in the homogenization is subdividing the fractured reservoir into two scales (see **Fig. 1**): local [small unit (SU)] scale of size (ℓ) and the global scale of size (L) that is much larger than the local scale. Our choice for the SU scale is a single matrix block surrounded by fractures, but it is also possible to choose a more complex structure with several matrix blocks for the SU scale. We define L as the dimension of the reservoir because the fractured reservoir of our choice is homogeneous in some averaged sense. However, if the fractured reservoir is locally heterogeneous, it is possible to define L as the dimension of the gridblock length. A very large difference between the size of the global scale (reservoir) and the local scale (SU), in addition to the low permeability of matrix blocks, suggests that the oil flux from the matrix blocks to fractures will lead only to local scale variations of the fracture potential. We define a scaling ratio $\varepsilon = \ell/L$ of the local scale to the global scale.

Therefore, we consider the medium as an aggregate of SU's, in which each unit cell consists of a matrix block surrounded by fractures. Fig. 1 also illustrates our assumption that the fractured reservoir consists of a continuous network of fractures with isolated matrix blocks in between. The SU is denoted as the domain $\Omega = \Omega_f \cup \Omega_m$ of which the fracture part is denoted as Ω_f and the matrix part as Ω_m.

The coordinates are denoted by $\mathbf{x}_b$ for the global scale and by $\mathbf{x}_s$ for the local scale. By letting ∂ denote *boundary of,* the matrix/fracture interface will be denoted by $\partial\Omega_m$. Let $\mathbf{n}$ denote the outward unit normal vector to this surface ($\partial\Omega_m$) pointing from the matrix to the fracture.

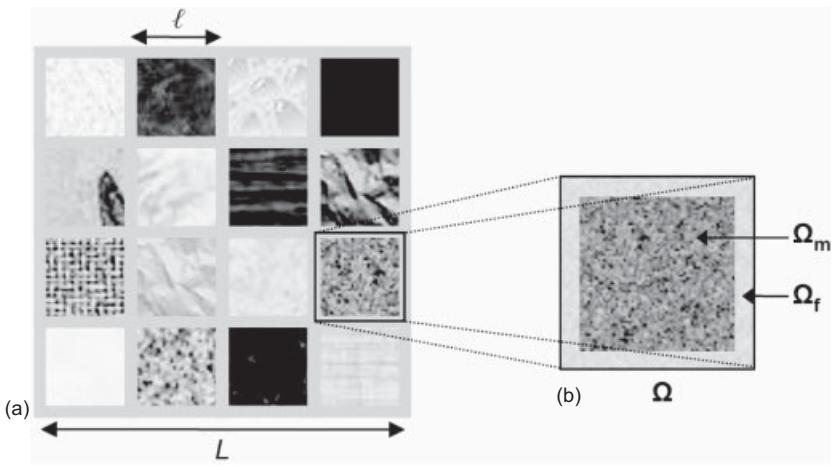

Fig. 1—The global scale (a) and the local scale (SU) (b).

The second step in homogenization is to describe the transport equations on the local scale (i.e., in fractures and matrix blocks):

$$\begin{aligned}\frac{\partial}{\partial t}\left(\phi_f^* \rho_{\alpha f} S_{\alpha f}\right) &= \nabla \cdot \left(\rho_{\alpha f} \lambda_{\alpha f}^* \nabla \Phi_{\alpha f}\right) \text{ in } \Omega_f, \\ \frac{\partial}{\partial t}\left(\phi_m \rho_{\alpha m} S_{\alpha m}\right) &= \nabla \cdot \left(\rho_{\alpha m} \lambda_{\alpha m} \nabla \Phi_{\alpha m}\right) \text{ in } \Omega_m\end{aligned} \quad \ldots\ldots\ldots\ldots\ldots (2)$$

These equations are found by combining the mass-balance equation and Darcy's equation. At the interface $\partial\Omega_m$, there is a continuity of oil and water flow:

$$\begin{aligned}&\left(\rho_{\alpha f} \lambda_{\alpha f}^* \nabla \Phi_{\alpha f}\right) \cdot \mathbf{n} = \left(\rho_{\alpha m} \lambda_{\alpha m} \nabla \Phi_{\alpha m}\right) \cdot \mathbf{n}, \\ &\text{and} \quad P_{cf}^*\left(S_{wf}\right) = P_{cm}\left(S_{wm}\right) \quad \text{on } \partial\Omega_m\end{aligned} \quad \ldots\ldots\ldots\ldots\ldots (3)$$

Indeed, there is a continuity of flux and capillary pressure at this interface unless one of the phases in the fracture or matrix system is immobile. Flux continuity follows from fluid conservation at the interface of fracture and matrix.

The third step is that the differentiation in the model equation is split into a global-scale (big) term, ∇_b, and a local-scale (small) term, ∇_s, where $\nabla = \nabla_b + \nabla_s$. The matrix equation acts at the local scale. Therefore, it is necessary to apply this splitting procedure only for the fracture equation. It is assumed that the contribution of differentiation at the local scale $\nabla_s(*)$ is one order of magnitude larger than the contribution of differentiation at the global scale $\nabla_b(*)$. In previous papers (Namdar Zanganeh et al. 2007; Bruining and Darwish 2006), we erroneously stated that these terms were of the same order of magnitude. However, this does not affect any of the results.

Subsequently, the transport equations are nondimensionalized by inspection (Shook et al. 1992). In the nondimensionalizing procedure, the first step is to write dependent and independent variables, X, as $X = X_R X_D + X_{\text{off}}$, where X_R is a reference quantity and X_{off} is an offset. The reference quantities assume values that can be indicated in the problem of interest or are made up by combining the reference quantities. In our model, we use ℓ and L, respectively, as the local and global reference (characteristic) lengths for differentiation. This results in $\nabla_D = \nabla_b + \varepsilon^{-1} \nabla_s$. The reference pressure, P_R, is the pressure difference between the injection and the production well (ΔP), k_R is the reference permeability, and $t_R = L^2 \mu_w / (k_R \Delta P)$ acts as the reference time for the fracture system. The new dimensionless potential (divided by p_R) is equal to the dimensionless pressure plus a rescaled gravity term: $\Phi_{\alpha f} = p_{\alpha f} + \rho_{\alpha f} g L z_D / \Delta P$, where z_D is the dimensionless vertical distance using L as the reference length. Eq. 2 has ρ_α as a common factor; therefore, it can be ignored in the nondimensionalization procedure.

Afterwards, the reference and other quantities in each of the terms are grouped such that a dimensionless equation is obtained. This procedure leads to a dimensionless equation (with dimensionless dependent and independent variables) with some dimensionless numbers such as the permeability ratio. This ratio is defined as the ratio of intrinsic fracture permeability to the matrix permeability. We will consider only a single case for the ratio of the fracture to matrix permeability (see subsection on permeability ratio). The other dimensionless number appearing in the equations is the scaling ratio ε. Different upscaled equations are obtained when dimensionless numbers assume values of different orders of magnitude with respect to ε. After nondimensionalizing Eq. 2, it reduces to

$$\begin{aligned}\frac{\partial}{\partial t}\left(\phi_f^* S_{\alpha f}\right) = \nabla_b \cdot \frac{k_f^* k_{r\alpha,f}}{\mu_{\alpha,f}} &\left(\nabla_b \Phi_{\alpha f} + \frac{1}{\varepsilon} \nabla_s \Phi_{\alpha f}\right) \\ + \frac{1}{\varepsilon} \nabla_s \cdot \frac{k_f^* k_{r\alpha,f}}{\mu_{\alpha,f}} &\left(\nabla_b \Phi_{\alpha f} + \frac{1}{\varepsilon} \nabla_s \Phi_{\alpha f}\right) \quad \text{in } \Omega_f\end{aligned} \quad \ldots\ldots (4)$$

The subscript D is dropped for reasons of concise notation.

In the same way, we derive Eq. 5 from the matrix equation (Eq. 2) by assuming that the differentiation with respect to the local scale is relevant only for the matrix equation and using the same reference time as in the fracture equation:

$$\frac{\partial}{\partial t}\left(\phi_m S_{\alpha m}\right) = \frac{1}{\varepsilon^2} \nabla_s \cdot \left(\lambda_{\alpha m} \nabla_s \Phi_{\alpha m}\right) \text{ in } \Omega_m. \quad \ldots\ldots\ldots\ldots\ldots (5)$$

At the interface $\partial\Omega_m$, there is a continuity of oil and water flux. The BC, Eq. 3, is rescaled similarly, i.e.,

$$k_f^* k_{r\alpha,f} \left(\nabla_b + \frac{1}{\varepsilon} \nabla_s\right) \Phi_{\alpha f} \cdot \mathbf{n} = k_m k_{r\alpha,m} \frac{1}{\varepsilon} \nabla_s \Phi_{\alpha m} \cdot \mathbf{n} \quad \text{on } \partial\Omega_m \quad \ldots\ldots\ldots (6)$$

In this contribution, we assume that the density and viscosity are uniform and constant.

In the fourth step, we expand the dependent variables into the contributions of decreasing significance with respect to ε:

$$\xi = \xi^{(0)} + \varepsilon \xi^{(1)} + \varepsilon^2 \xi^{(2)} + \ldots, \quad \ldots\ldots\ldots\ldots\ldots (7)$$

where ξ denotes either the saturation or the potential. Substitution of these series into the dimensionless equations results in equations consisting of terms with different orders of magnitude with respect to ε (Eq. 7 is substituted into Eqs. 4 through 6). Because the upscaling procedure should also be valid for ε values that are slightly smaller or larger, it is stated that each of the terms with a specific order of ε constitutes an equation that is separately satisfied. First, the equation of the lowest order in ε is solved, leading to the solutions of the most significant contributions of the dependent variables. This means that the $1/\varepsilon^2$ terms of Eq. 4 and the $1/\varepsilon$ term of Eq. 6 with Eq. 7 lead, respectively, to

$$\begin{aligned}&\frac{1}{\varepsilon^2} \nabla_s \cdot k_{r\alpha,f}^{(0)} \nabla_s \Phi_{\alpha f}^{(0)} = 0 \quad \text{in } \Omega_f \\ &\text{and} \quad \frac{1}{\varepsilon} k_{r\alpha,f}^{(0)} \nabla_s \Phi_{\alpha f}^{(0)} \cdot \mathbf{n} = 0 \quad \text{on } \partial\Omega_m\end{aligned}, \quad \ldots\ldots\ldots\ldots\ldots (8)$$

where we used the fact that $k_f^*/k_m \sim 1/\varepsilon^2$. Assuming periodic boundary conditions, Eq. 8 has a unique solution for each part, which ensures that each phase potential is constant on the local scale. Indeed, a constant phase potential is periodic and satisfies the system of Eq. 8. Under static conditions (see, however, Hassanizadeh et al. 2002), this would mean that there is capillary/gravity equilibrium in the SU, unless one of the phases is immobile.

Subsequently, it is possible to show that the equation with one order higher in ε (ε^{-1} terms of Eq. 4 and ε^0 terms of Eq. 6) is a linear elliptic problem for $\nabla_s \Phi_{\alpha f}^{(1)}$ in terms of $\nabla_s \Phi_{\alpha f}^{(0)}$. Constructing a relation between these two terms gives another system of differential equations that can be used to estimate $\Phi_{\alpha f}^{(1)}$ (see Appendix A). The third system (ε^0 terms of Eq. 4 and ε^1 terms of Eq. 6) is the most important system because when averaged, it gives the most significant upscaled model:

$$\begin{aligned}\frac{\partial}{\partial t}\left(\phi_f^* S_{\alpha f}^{(0)}\right) = \nabla_b \cdot \frac{k_f^* k_{r\alpha,f}^{(0)}}{\mu_{\alpha,f}} &\left[\nabla_b \Phi_{\alpha f}^{(0)} + \nabla_s \Phi_{\alpha f}^{(1)}\right] \\ + \nabla_b \cdot \frac{k_f^* k_{r\alpha,f}^{(1)}}{\mu_{\alpha,f}} &\nabla_s \Phi_{\alpha f}^{(0)} \\ + \nabla_s \cdot \frac{k_f^* k_{r\alpha,f}^{(0)}}{\mu_{\alpha,f}} &\left[\nabla_b \Phi_{\alpha f}^{(1)} + \nabla_s \Phi_{\alpha f}^{(2)}\right] \\ + \nabla_s \cdot \frac{k_f^* k_{r\alpha,f}^{(1)}}{\mu_{\alpha,f}} &\left[\nabla_b \Phi_{\alpha f}^{(0)} + \nabla_s \Phi_{\alpha f}^{(1)}\right] \\ + \nabla_s \cdot \frac{k_f^* k_{r\alpha,f}^{(2)}}{\mu_{\alpha,f}} &\nabla_s \Phi_{\alpha f}^{(0)} \\ &\text{in } \Omega_f\end{aligned} \quad \ldots\ldots\ldots\ldots\ldots (9)$$

The corresponding BC with terms ε^1 reads

$$\frac{k_f^* k_{r\alpha,f}^{(0)}}{\mu_{\alpha,f}}\left[\nabla_b \Phi_{\alpha f}^{(1)} + \nabla_s \Phi_{\alpha f}^{(2)}\right]\cdot \mathbf{n} + \frac{k_f^* k_{r\alpha,f}^{(1)}}{\mu_{\alpha,f}}\left[\nabla_b \Phi_{\alpha f}^{(0)} + \nabla_s \Phi_{\alpha f}^{(1)}\right]\cdot \mathbf{n}. \quad \ldots\ldots\ldots\ldots\ldots\ldots\ldots (10)$$

$$= \frac{1}{\varepsilon^2}\frac{k_m k_{r\alpha,m}^{(0)}}{\mu_{\alpha,m}}\nabla_s \Phi_{\alpha m}^{(0)}\cdot \mathbf{n} \quad \text{on } \partial\Omega_m$$

It is possible to average the equations over an SU. Here, we use the notation $\langle \mathbf{q} \rangle$ for the spatial average of any parameter $\mathbf{q}$, over an SU, i.e.,

$$\langle q \rangle = \frac{1}{|\Omega|}\int_{\Omega_f} \mathbf{q}\, d\mathbf{x}_s. \quad \ldots\ldots\ldots\ldots\ldots\ldots\ldots\ldots\ldots\ldots (11)$$

In particular, considering the assumption of periodic local variations, the application of the Gauss theorem leads to

$$\frac{1}{|\Omega|}\int_{\Omega_f} \nabla_s \cdot \mathbf{q}\, d\mathbf{x}_s = -\frac{1}{|\Omega|}\int_{\partial\Omega_m} \mathbf{q}\cdot \mathbf{n}\, d\sigma$$
$$= -\frac{1}{|\Omega|}\int_{\Omega_m} \nabla_s \cdot \mathbf{q}\, d\mathbf{x}_s \quad \ldots\ldots\ldots\ldots\ldots\ldots\ldots (12)$$

In this equation, σ denotes the coordinates of the boundary, $\partial\Omega_m$. Note that $\mathbf{n}$ is the outward unit normal vector to this surface ($\partial\Omega_m$) pointing from the matrix to the fracture. The contributions from the outer boundary of Ω cancel because $\mathbf{q}$ is considered Ω-periodic.

We obtain the averaged 0th-order upscaled equation in three steps. First, we apply Eq. 12 to Eqs. 5, 9, and 10. Then, we consider that the terms containing $\nabla_s \Phi_{\alpha m}^{(0)}$ are zero; and last, we substitute Eqs. 10 and 5 into Eq. 9:

$$\frac{\partial}{\partial t}\left[\phi_f S_{\alpha f}^{(0)}\right] + \frac{\partial}{\partial t}\frac{1}{|\Omega|}\int_{\Omega_m}\left[\phi_m S_{\alpha m}^{(0)}\right] d\mathbf{x}_s$$
$$= \nabla_b \cdot \frac{k_f k_{r\alpha,f}^{(0)}}{\mu_{\alpha,f}}\nabla_b \Phi_{\alpha f}^{(0)} \quad \text{in } \Omega_f \quad \ldots\ldots\ldots\ldots\ldots\ldots\ldots (13)$$

where we derived the effective-fracture-permeability tensor (see Appendix A) and the global fracture porosity, as follows:

$$k_f = \frac{1}{|\Omega|}\int_{\Omega_f} k_f^*\left(\mathbf{I} + \nabla_s \otimes \omega\right) d\mathbf{x}_s, \quad \text{and} \quad \phi_f = \frac{|\Omega_f|}{|\Omega|}\phi_f^*. \quad \ldots\ldots\ldots\ldots\ldots\ldots\ldots (14)$$

The dyadic product $\nabla_s \otimes \omega$ is a tensor with components $\partial\omega_j / \partial x_i$ where i,j denote the x, y, z coordinates. Arbogast (1993) has derived similar equations for special cases previously. The 0th-order upscaled equation (Eq. 13) describes the global displacement process through a globally equivalent homogeneous medium characterized by effective coefficients (i.e., ϕ_f and k_f).

Dimensionless Numbers

One of the advantages of homogenization is that it generates different upscaled models when characteristic dimensionless numbers assume values of different orders of magnitude with respect to ε. In this case, where we are dealing only with the 0th-order upscaled equation, we use the ratio of the fracture permeability to the matrix permeability as the characteristic dimensionless number. Other dimensionless numbers follow from the upscaled model equations. For these equations, we can additionally define the gravity number (i.e., gravity force over viscous force) and the Peclet number. The Peclet number is defined as the ratio between the time required to imbibe water into the matrix block and the travel time of water in the fracture system. Here, all relevant dimensionless numbers playing a role both in the upscaling procedure and in the ensuing model equations are discussed.

Permeability Ratio in Fractures and Matrix. The simplest definition of a fractured medium is a medium that contains fractures and matrix blocks. From the fluid-flow point of view, such a medium is not necessarily a fractured medium, in particular when the matrix blocks carry a substantial part of the flow. A fractured reservoir from the fluid-flow point of view means that the total volumetric flux u_f in fractures must be substantially larger than the total volumetric flux u_m in the matrix blocks. It can be shown that the necessary requirement for this is that $k_f^* \sim \varepsilon^{-2} k_m$. Indeed, flows in the fracture and matrix are subjected to approximately the same potential gradient. In addition, the fluid viscosities in the matrix and fracture are the same. Hence, the ratio of the velocity in the fracture to that in the matrix u_f^*/u_m is of the order $\sim \varepsilon^{-2}$. For a statistically homogeneous medium, the Darcy velocity is $u_f \sim \phi_f u_f^*$. Because in our case the global fracture porosity (ϕ_f) is of the order $\sim \varepsilon$, we obtain $u_f/u_m \sim \varepsilon^{-1}$. This can be expressed in terms of permeabilities (i.e., $k_f/k_m \sim \varepsilon^{-1}$), using Darcy's law. This means that if the matrix permeability is 10 md and $\varepsilon \sim 0.01$, the intrinsic fracture permeability k_f^* must be on the order of 100 darcies. The order of magnitude of the permeability ratio also has a consequence for a number of other aspects in fractured media flow. If we assume that the capillary pressure is inversely proportional to the square root of the permeability, $\sqrt{k}$, it means that for the same saturation values the capillary pressure in the matrix blocks is 100 times as large as that in the fracture.

Peclet Number. The Peclet number is defined as the ratio of the time required to imbibe water into the matrix block to the travel time of water in the fracture system. The derived Peclet number is based on inspection [i.e., a dimensional analysis of the model equations used (Shook et al. 1992)]. For our model, we assume that countercurrent imbibition in the matrix is the main recovery mechanism. Flow in the fractures is governed by multiphase convection flows. Therefore, in this model, the Peclet number expresses the ratio of transport by convection (mainly viscous forces) in the fracture to the transport by capillary diffusion in the matrix. For other cases of interest, the relevant dimensionless number can be derived from the ratios of the residence time of the fluids in the matrix blocks and fractures, respectively. For our situation, we derive the following expressions for the Peclet number:

$$\mathrm{Pe} = \frac{\ell^2 u_f}{D_{\mathrm{cap}} L}, \quad \text{where} \quad D_{\mathrm{cap}} = -\frac{\lambda_o \lambda_w}{\lambda_o + \lambda_w}\frac{dP_c}{dS_w}. \quad \ldots\ldots\ldots (15)$$

Here λ_α is the mobility of phase α (oil, water), ℓ is the matrix block size, and L is the distance between wells. We use u_f on the basis of some of our simulations, although we admit that the best choice of u_f or u_f^* depends on the situation. The qualitative behavior of waterdrive recovery in fractured media depends on the ratio of the characteristic time over which an amount of oil flows from the matrix to the fracture and the residence time of water in the fracture system.

If the residence time in the fracture system is small, it is expected that the recovery is controlled by the rate of countercurrent imbibition from the matrix blocks. In this case, most of the fractures contain mainly water. By capillary continuity, this sets the boundary of the matrix blocks at approximately zero capillary pressure.

If the residence time in the fracture system is large, water imbibes into the matrix blocks before reaching the production well and releases an equal volume of oil (in the case of incompressible flow) to the fracture. In this case, there is a long period in which mainly oil is produced at a rate equal to the injection rate with little water. After this period, water breakthrough occurs and the production performance depends on the detailed geometry of the fracture system and the well configurations. Therefore, from

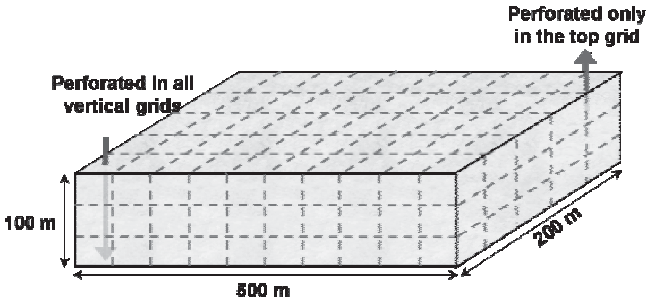

Fig. 2—Reservoir waterflooding pattern and geometry in the numerical example.

the fluid-flow point of view, the fractured reservoir behaves like a highly heterogeneous single-porosity reservoir rather than a dual-porosity fractured reservoir. The heterogeneity distribution must be inferred from the properties of the fracture system.

Ratio of Gravity to Viscous Forces (Gravity Number). The gravity number is defined as the ratio of the gravity forces to the viscous forces. For the 0th-order model, the periodic BC implies that viscous forces are negligible with respect to gravity forces or capillary forces on the scale of the matrix blocks. Therefore, we define the gravity number on the global (reservoir) scale. The 0th-order model follows from the most significant terms in the transport equations (i.e., those that scale with ε^0). We assert that this model is sufficiently accurate to grasp the essential features of flow in fractured reservoirs.

The gravity number is defined as

$$N_G = \frac{k_f^* \Delta\rho\, gH}{\mu\, u_f^* L}, \quad \ldots\ldots\ldots\ldots\ldots\ldots\ldots\ldots\ldots\ldots\ldots\ldots (16)$$

where H is the height of the reservoir. Considering that capillary diffusion transport is known, the Peclet number is specified by the viscous forces in the fracture system. If the Peclet number is large, the viscous forces of the fracture system dominate gravity forces in the fracture system. On the other hand, when the Peclet number is small and injection is over the entire height of the reservoir, gravity forces become dominant in the fracture system. This means that for this case, water tends to underride, especially for high mobility ratios, and gravity segregation happens.

Results and Discussion

This section compares the results between the homogenized model, the effective permeability model (obtained from homogenization), and computations by ECLIPSE, which are based on the WR model. Appendix A describes the derivation of the effective permeability, and Appendix B describes the numerical homogenized model. The homogenized model (see **Fig. 2**) contains 10 gridblocks in the x-direction, five gridblocks in the y-direction, and three gridblocks in the z-direction. The matrix in each gridblock is represented by a single representative matrix block, which is in turn discretized into 9×9×9 gridblocks. In other words, we use 109,500 gridblocks for the homogenized model. The effective permeability model and ECLIPSE also use a discretization into 10×5×3 gridblocks. **Table 1** gives the data used to compare the homogenized model, the effective-permeability model, and ECLIPSE. **Fig. 3** shows the capillary pressure curve for matrix and fracture, and **Fig. 4** shows oil and water relative permeability curves for matrix and fracture.

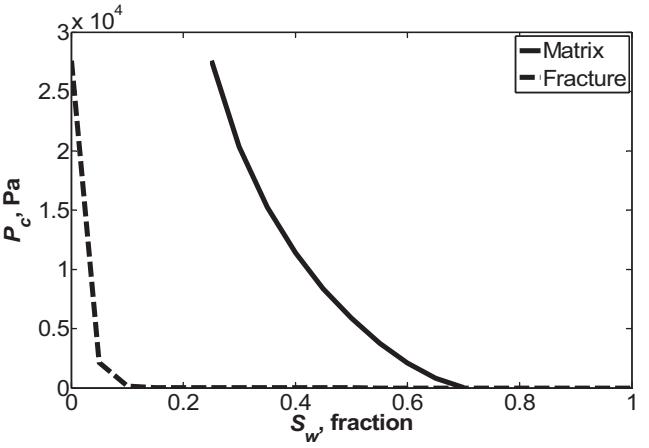

Fig. 3—Capillary pressure curve for fracture and matrix.

In the simulations, we vary the Peclet number (rate of water injection), while keeping the other properties constant. In all the cases, cumulative oil and water productions are the basis for comparison. The cumulative-production curve can be differentiated with respect to time to give the production rates at any time. We also investigate the effect of fracture-gridblock refinement on

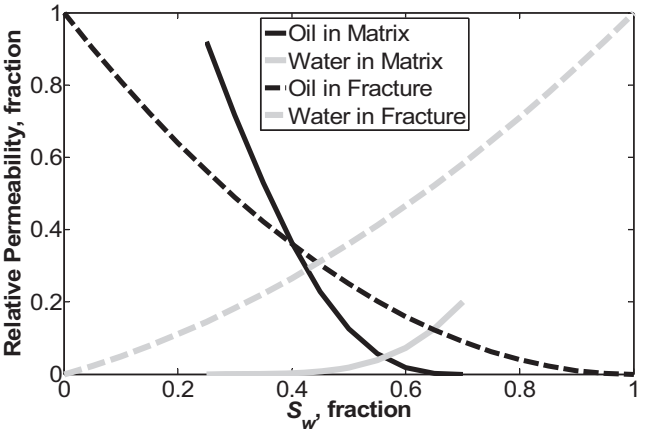

Fig. 4—Oil and water relative permeability curves for matrix and fracture.

TABLE 1—DATA USED IN THE SIMULATIONS

Initial reservoir pressure (MPa)	27.5	Matrix permeability, k_m (md)	1
Bottom hole pressure for production wells (MPa)	26.9	Oil viscosity, μ_o (Pa.s)	0.002
Well radius (m)	0.1524	Oil density, ρ_o (kg/m^3)	833
Fracture aperture (μm)	100	Water viscosity, μ_w (Pa.s)	0.0005
Local fracture porosity, ϕ_f^*	1	Water density, ρ_w (kg/m^3)	1025
Intrinsic fracture permeability, k_f^*(D)	844	Oil residual saturation in matrix	0.3
Global fracture porosity, ϕ_f	1.5×10^{-4}	Oil residual saturation in fracture	0
Effective fracture permeability, k_f(md)	84.43	Connate water saturation in matrix	0.25
Matrix block size, l (m)	2	Connate water saturation in fracture	0
Matrix porosity, ϕ_m	0.19		

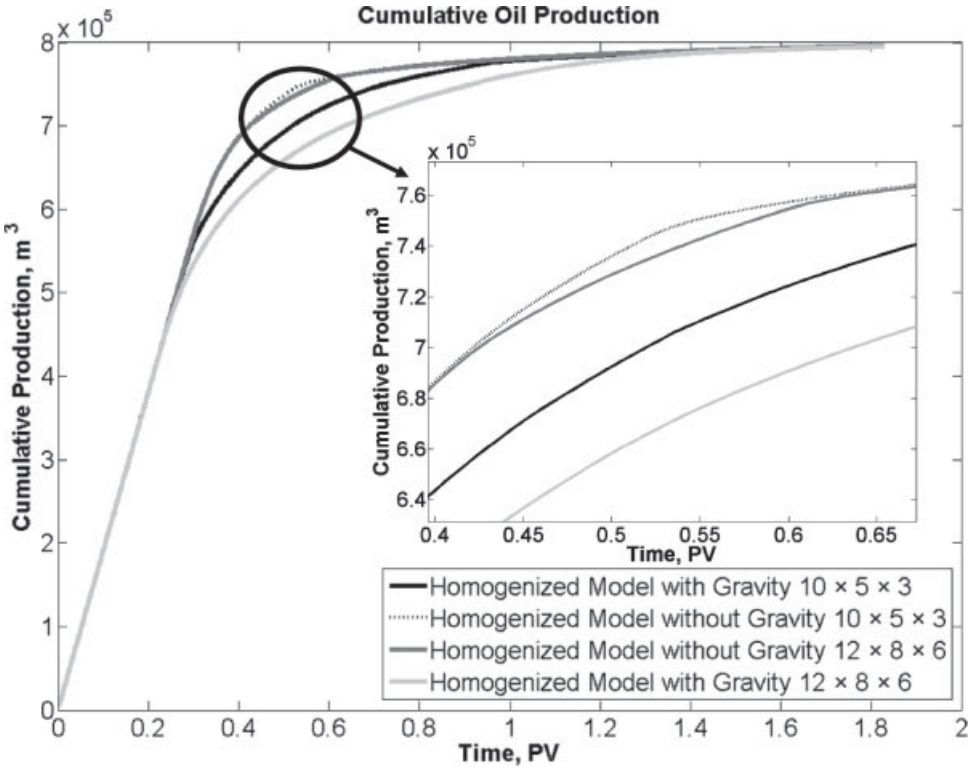

Fig. 5—Effects of fracture-gridblock refinement on the cumulative oil production.

the results in a case where we anticipate the highest degree of sensitivity to gridblock refinement [Pe = 0.77, $N_G = 0.14$, $q_w = 0.1$ pore volume (PV) per year]. Results (see **Fig. 5**) suggest that the choice of 10×5×3 is somewhat coarse for accurate results when gravity is included but is still sufficient for making comparison between the models. Note that the scale in Fig. 5 differs from that in the subsequent figures.

Figs. 6a through 6d show a comparison of the cumulative oil and water production for the homogenized case and the effective-permeability case. For a low Peclet number (0.21) (Fig. 6a), we observe that the homogenized model initially predicts lower production, but it predicts larger oil production when more than 80% of 1 PV is injected. At a slightly higher Peclet number (Fig. 6b), we observe that the homogenized model and effective-permeability model almost coincide. At higher Peclet numbers (Figs. 6c and 6d), the discrepancy between the homogenized model and the effective-permeability model increases, where the homogenized model predicts a recovery that is almost two times smaller.

If the Peclet number is small, the rate of oil and water exchange at the interface of matrix block and fracture is rapid compared to the rate of convection in the fractures. In this case, the residence time in the fracture system is large and most water imbibes into the matrix blocks and releases an equal volume of oil to the fracture. Therefore, there is a long period when mainly oil is produced at a rate equal to the injection rate, with only little water (Fig. 6a). Note that for the effective-permeability model, we solved the equations that correspond to a single conventional porosity model, with porosity equal to the matrix porosity and permeability equal to the effective permeability obtained from homogenization. In other words, in this case, we did not consider both the fracture system and the matrix system simultaneously. Therefore, the computation time of the effective-permeability model is a few hundred times smaller than that of the homogenized model.

On the other hand, if the Peclet number is large, the rate of oil and water exchange at the interface of the matrix block and the fracture is small compared to the rate of convection in the fractures. Consequently, the residence time in the fracture system is small. Therefore, it is expected that the recovery is controlled by the rate of countercurrent imbibition from the matrix blocks. In this case, most of the fractures contain mainly water. By capillary continuity, this situation sets the boundary of the matrix blocks at the approximately zero capillary pressure, leading to a water saturation of $1-S_{or}$. As a result of this, there is a short period in which mainly oil is produced (Fig. 6d) after which oil production becomes very slow.

Note that at very low Peclet numbers (Fig. 6a), the discrepancy between the homogenized model and the effective-permeability model is larger than for intermediate Peclet numbers (Fig. 6b). This is attributed to gravity segregation, as discussed in the section, Ratio of Gravity to Viscous Forces (Gravity Number).

Figs. 7a through 7d show a comparison of the cumulative oil and water production for the homogenized model and ECLIPSE simulator. For a small Peclet number (0.21, as in Fig. 7a), at an early stage ($t < 0.25$ PV), the cumulative oil and water production for both the homogenized model and the ECLIPSE simulator are the same. At the intermediate stage (0.25 PV $< t <$ 0.6 PV), the homogenized model predicts lower oil production than ECLIPSE. Subsequently, at $t > 0.6$ PV, the homogenized model predicts a higher oil production than the ECLIPSE simulator, as illustrated by the fact that the slope of cumulative-oil-production curve for the homogenized model at this stage is steeper than the slope of the cumulative-oil-production curve for ECLIPSE. Finally, both the homogenized-model and the ECLIPSE results tend to the same values of water and oil production. The discrepancy in Fig. 7a between the homogenized model and ECLIPSE is caused by the large gravity effects, which requires again an accurate representation of the matrix/fracture interaction. For slightly higher Peclet number (Fig. 7b), we see that the cumulative oil and water production for the homogenized model and ECLIPSE simulator almost coincide. Therefore, in this condition the homogenized model can be replaced by the WR approach without appreciable loss of accuracy.

The results at still higher Peclet numbers are shown in Figs. 7c and 7d. In these cases, the homogenized model predicts a higher oil production at an early stage than the ECLIPSE simulator because of depletion of oil from the part of the matrix block adjacent to the fracture resulting from continuity of capillary pressure. Afterwards, the predicted rate of oil production of ECLIPSE exceeds the rate of oil production of the homogenized model, and gradually the cumulative oil and water production from the ECLIPSE simulator reaches the value of the cumulative oil and water production for the homogenized model. For Pe = 8.41, this was observed only after 5 PV of water injection (not shown in Fig. 7d).

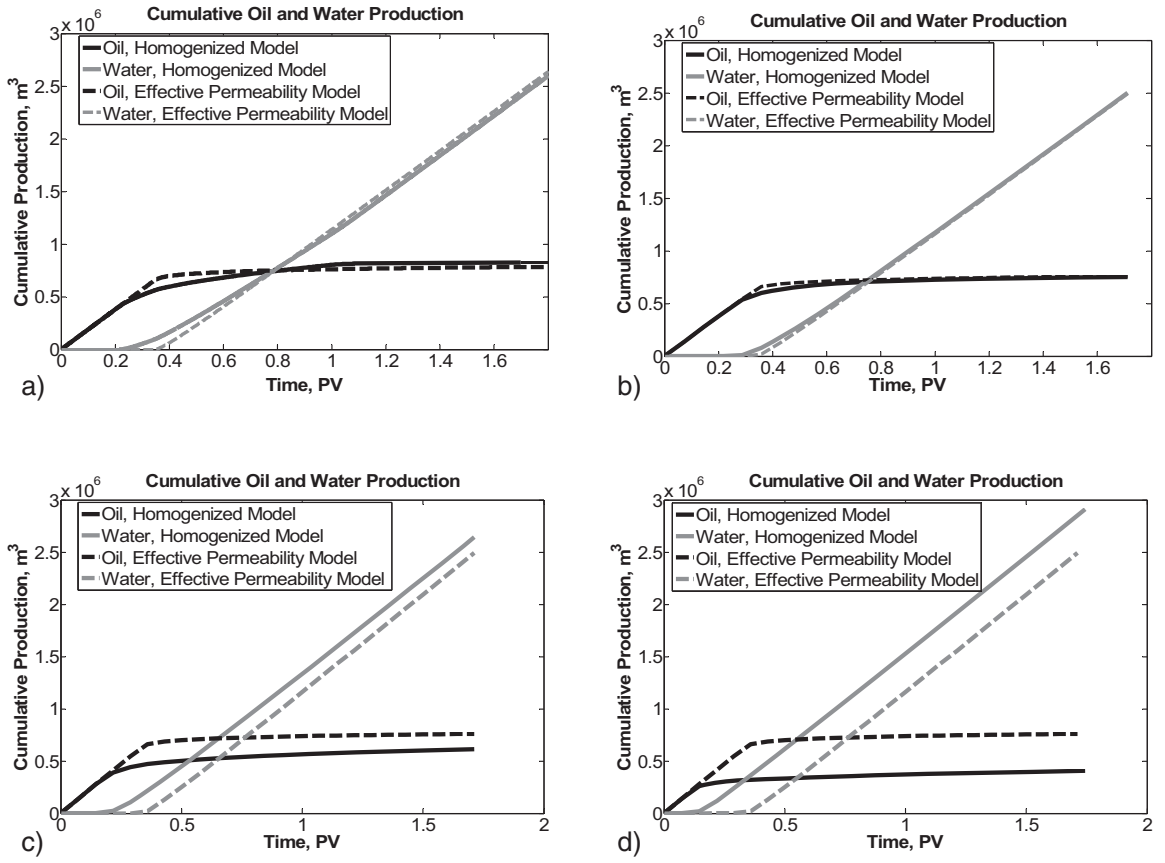

Fig. 6—(a) *Pe* = 0.21, q_w = 0.01 PV/yr, and K_m = 1 md; (b) *Pe* = 1.19, q_w = 0.5 PV/yr, and K_m = 1 md; (c) *Pe* = 8.41, q_w = 5.0 PV/yr, K_m = 1 md; and (d) *Pe* = 1,728, q_w = 100.0 PV/yr, and K_m = 1 md.

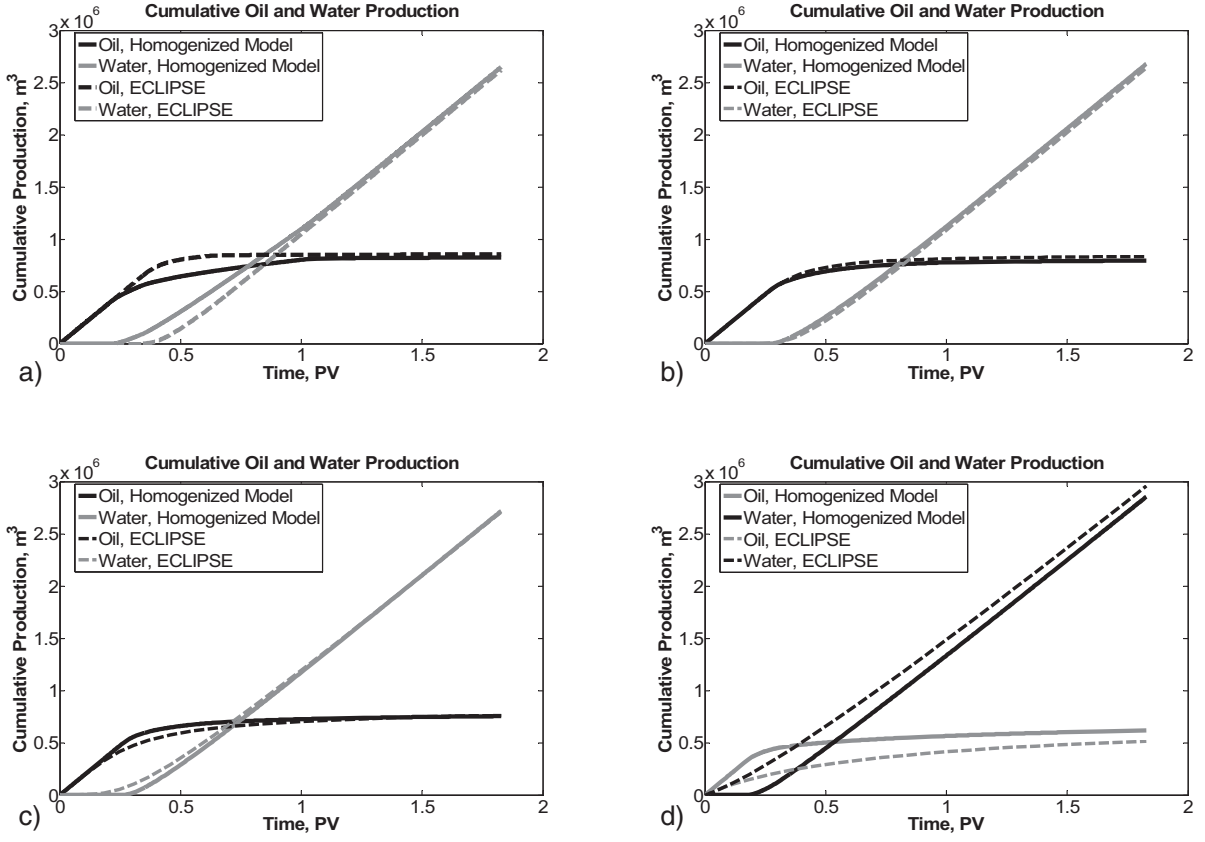

Fig. 7—(a) *Pe* = 0.21, q_w = 0.01 PV/yr, and K_m = 1 md; (b) *Pe* = 0.77, q_w = 0.1 PV/yr, and K_m = 1 md; (c) *Pe* = 1.19, q_w = 0.5 PV/yr, K_m = 1 md; and (d) *Pe* = 8.41, q_w = 5.0 PV/yr, and K_m = 1 md.

The most important reason for the discrepancy between the homogenized model and the ECLIPSE model is the difference between the WR transfer function and the transfer function based on homogenization. The second-most-important reason is that 3D matrix-block subgridding to the best of our knowledge is not available in the ECLIPSE simulator. We observe that most of the discrepancy between the homogenized model and ECLIPSE simulator happens at a higher Peclet number. In this case, accurate transfer functions are necessary for the accurate prediction of oil recovery because the oil recovery is controlled by the rate of countercurrent imbibition. Consequently, satisfying the continuity of the capillary pressure has a significant effect on the cumulative oil and water production.

As in Fig. 6a, at very small Peclet numbers (Fig. 7a), the discrepancy between the homogenized model and ECLIPSE is larger than for intermediate Peclet numbers (Figs. 7b and 7c).

Figs. 6a, 6b, 7b, and 7c show a very small difference between the homogenized model and the effective-permeability model and ECLIPSE. We explain this observation using two different regimes based on the magnitude of the Peclet number (small or large). When the Peclet number is small but not so small that gravity starts to dominate, the rate of fluid transport in the fracture controls the oil recovery mechanism. Therefore, in this regime, considering a precise rate of fluid exchange at the interface of matrix and fracture is not required for the prediction of oil-recovery from waterflooded fractured reservoirs. For this reason, one can use either the effective-permeability model (see Figs. 6a and 6b) or the WR approach (see Figs. 7b and 7c) instead of using the homogenized model. Hence, when the Peclet number is small (Pe < 1), but not so small that gravity starts to dominate, we can use either the effective-permeability model (Figs. 6a and 6b) or the WR approach (Figs. 7b and 7c) instead of using the homogenized model. Note that the effective-permeability model does not have an exchange term because it is a single-porosity model. Therefore, it can be implemented easily and has a very small computational time compared to the other two models. On the other hand, there is a critical Peclet number marking the boundary between the two regimes. If the Peclet number is large (as in Figs. 6c, 6d, and 7d), there is a large difference between the homogenized model and either the effective-permeability model or the WR approach. In this regime, the oil-recovery mechanism is controlled by the rate of countercurrent imbibition from the matrix blocks. In this case, the exchange rate between matrix and fracture is described better by the physically based homogenization approach than by the semi-empirical WR approach. Therefore, we must use the homogenized model when the Peclet number is large.

A comparison of the cumulative oil and water production for the homogenized model with gravity and the homogenized model without gravity is shown in **Figs. 8a through 8d.** For small Peclet number and large gravity number (N_G=1.51), it can be seen from Fig. 8a that at an early stage both the homogenized model with gravity and the homogenized model without gravity predict the same oil production, but later on water breakthrough occurs earlier for the homogenized model with gravity and hence leads to less oil production. When gravity is included in the model, underriding of water occurs. At a slightly higher Peclet number (0.77) and smaller gravity number (0.14) (see Fig. 8b), we observe that the effect of gravity becomes smaller and for much higher Peclet numbers and much smaller gravity numbers (Figs. 8c and 8d) and the results of the homogenized model with gravity and the homogenized model without gravity almost coincide. The relatively small effect of gravity can be attributed to the fact that both capillary imbibition forces and viscous forces act against gravity forces. The capillary imbibition forces are constant for every case considered here. Moreover, gravity forces are also constant because the size of the reservoirs and the density difference between oil and water are kept constant. The viscous forces change on the global scale because we vary the rate of water injection for each Peclet number. When

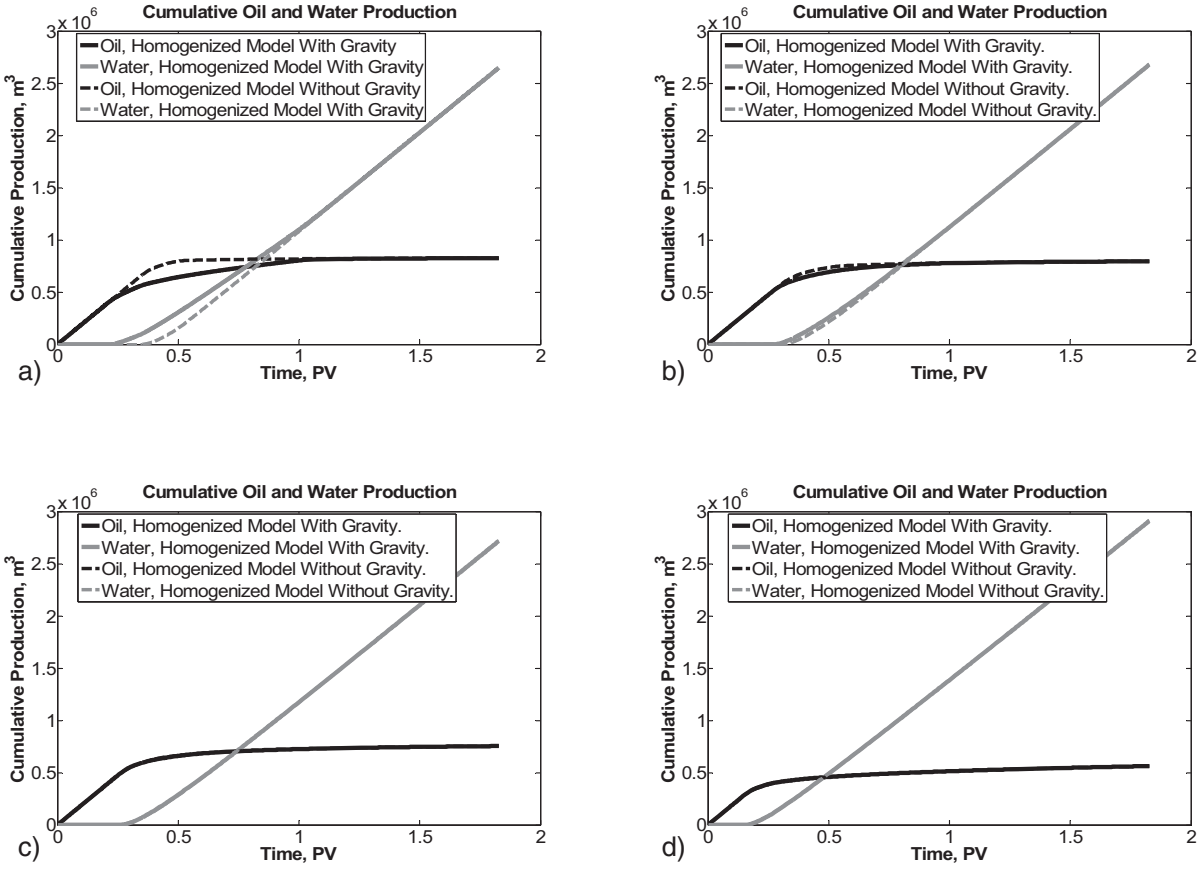

Fig. 8—(a) *Pe* = 0.21, N_G = 1.51, and q_w = 0.01 PV/yr; (b) *Pe* = 0.77, N_G = 0.14, and q_w = 0. 1 PV/yr; (c) *Pe* = 1.19, N_G = 0.03, and q_w = 0.5 PV/yr; and (d) *Pe* = 20.31, N_G = 0.001, and q_w = 10.0 PV/yr.

the Peclet number is small and gravity number is large, the viscous forces are small and therefore the effects of gravity forces can be observed. On other hand, at high Peclet numbers and very small gravity number, the viscous forces are at least one order of magnitude larger than gravity forces. Hence, the viscous forces become dominant and considering gravity forces for these cases does not have a large impact on the cumulative oil and water production. This is based on a geometry that we consider here.

Conclusions

- Homogenization does not require intuitive closure relations, but requires order-of-magnitude estimates of the characteristic (dimensionless) numbers to obtain the upscaled equations.
- In general, homogenization is an upscaling method with the advantage that it finds an appropriate upscaled equation for each parameter subspace in which the characteristic dimensionless numbers assume values of a certain order of magnitude with respect to the upscaling factor.
- The most important dimensionless numbers are (a) the ratio of fracture permeability to matrix permeability and (b) the Peclet number, which describes the ratio of countercurrent imbibition time to residence time of water in the fractures. A requirement for a dual-porosity model to be valid is that the intrinsic fracture permeability is two orders of magnitude larger with respect to the scaling factor than the matrix permeability.
- We derived a fully implicit 3D numerical model for the homogenized equations and implemented the numerical model in a computer code.
- The results show that:
  a. The discrepancy between an effective-permeability (homogeneous) model and a dual-porosity homogenized model increases from negligible at low, but not so low that gravity dominates, Peclet numbers to increasingly significant at higher Peclet numbers.
  b. A comparison with commercial software (ECLIPSE) shows that also only at low Peclet numbers, there is good agreement between the simulator and our numerical results.
  c. Gravity forces at high Peclet numbers and low gravity numbers do not have a large impact on the cumulative oil and water production.
- In view of its physical basis, we assert that improved fracture modeling can be achieved using homogenization.
- The homogenized model represents the physics of the problem better than the WR approach or the effective-permeability model, which is actually a single-porosity model. However, the computations with the homogenized model are time consuming, as explained in Appendix B. Therefore, it is important to discern the condition (i.e., the Peclet number) when the effective-permeability model can replace the homogenized model without appreciable loss of accuracy. For those conditions, the WR approach also gives accurate results.

Nomenclature

D_{cap} = capillary-diffusion coefficient
g = gravity acceleration
H = height of the reservoir
k = permeability
ℓ = matrix-block size
L = gridblock size or reservoir length
$\mathbf{n}$ = outward unit normal vector
N_G = gravity number
p_c = capillary pressure
P = pressure
q = any parameter or water-injection rate
S = saturation
S_{or} = residual-oil saturation
t = time
u = velocity
$\mathbf{u}$ = velocity vector
$\mathbf{x}_b$ = global coordinate
$\mathbf{x}_s$ = local coordinate
X = dependent or independent variable
z = vertical-upward direction
α = phase (oil/water)
ε = scaling ratio
λ = fluid relative mobility
μ = viscosity
ξ = potential/saturation indicator
ρ = density
σ = coordinates of the boundary
ϕ = porosity
Φ = potential
Ω = domain
ω = auxiliary function

Math Signs and Operator

$< >$ = average sign over volume
$| |$ = absolute value of volume
$\sim$ = same order of magnitude
$\otimes$ = dyadic product
$\sqrt{}$ = square root
$\int$ = integral
d = differential
∂ = partial differential
∇ = del (gradient operator)
Δ = delta (difference operator)
$\nabla\cdot$ = divergence operator
$\cup$ = union

Subscripts

b = global (big) index
D = dimensionless
f = fracture
m = matrix
o = oil phase
off = offset
r = relative
R = reference
s = local (small) index
w = water phase
α = oil/water index
ζ = fracture/matrix index

Superscripts

$*$ = local fracture index
(0) = 0th-order index
(1) = first-order index
(2) = second-order index

Acknowledgments

We thank William R. Rossen for insightful discussions and carefully reading the final manuscript. We acknowledge Maryam Namdar Zanganeh, Stefan Luthi, and Giovanni Bertotti for many useful discussions and comments. We also thank Statoil for supporting this work. We also acknowledge Sharif University of Technology for their steady collaboration.

References

Arbogast, T. 1993a. Gravitational forces in dual-porosity systems: I. Model derivation by homogenization. *Transport in Porous Media* **13** (2): 179–203. doi: 10.1007/BF00654409.

Arbogast, T. 1993b. Gravitational forces in dual-porosity systems: II. Computational validation of the homogenized model. *Transport in Porous Media* **13** (2): 205–220. doi: 10.1007/BF00654410.

Arbogast, T. 1997. Computational Aspects of Dual-Porosity Models. In *Homogenization and Porous Media*, ed. U. Hornung, Vol. 6, 203–223. New York City: Interdisciplinary Applied Mathematics, Springer-Verlag.

Arbogast, T. and Lehr, H.L. 2006. Homogenization of a Darcy-Stokes system modeling vuggy porous media. *Computational Geosciences* **10** (3): 291–302. doi: 10.1007/s10596-006-9024-8.

Barenblatt, G.I., Patzek, T.W., and Silin, D.B. 2002. The Mathematical Model of Non-Equilibrium Effects in Water-Oil Displacement. Paper SPE 75169 presented at the SPE/DOE Improved Oil Recovery Symposium, Tulsa, 13–17 April. doi: 10.2118/75169-MS.

Barenblatt, G.I., Zheltov, Iu.P., and Kochina, I.N. 1960. Basic concepts in the theory of seepage of homogeneous liquids in fissured rocks. *J. of Applied Mathematics and Mechanics* **24** (5): 1286–1303. doi: 10.1016/0021-8928(60)90107-6.

Bear, J. and Verruijt, A. 1987. *Modeling Groundwater Flow and Pollution*. Dordrecht, The Netherlands: Kluwer Academic Publishers.

Bruining J. and Darwish, M.I.M. 2006. Homogenization for Fe^{2+} Deposition Near Drink Water Tube Wells During Arsenic Remediation. Paper P003 presented at the European Conference on the Mathematics of Oil Recovery (ECMOR X), Amsterdam, 4–7 September.

Douglas, J. and Arbogast, T. 1990. Dual-Porosity Models for Flow in Naturally Fractured Reservoirs. In *Dynamics of Fluids in Hierarchical Porous Media*, ed. J.H. Cushman, 177–221. London: Academic Press.

Douglas, J. Jr., Arbogast, T., and Paes Leme, P.J. 1989. Two Models for Waterflooding of Naturally Fractured Reservoirs. Paper SPE 18425 presented at the SPE Symposium on Reservoir Simulation, Houston, 6–8 February. doi: 10.2118/18425-MS.

Douglas, J. Jr., Hensley, J.L., and Arbogast, T. 1991. A dual-porosity model for waterflooding in naturally fractured reservoirs. *Computer Methods in Applied Mechanics and Engineering* **87** (2–3): 157–174. doi: 10.1016/0045-7825(91)90004-P.

Dutra, T.V. Jr. and Aziz, K. 1992. A New Double-Porosity Reservoir Model for Oil/Water Flow Problems. *SPE Res Eng* **7** (4): 419–425. SPE-21248-PA. doi: 10.2118/21248-PA.

Gasem, F.H., Nashawi, I.S., Gharbi, R., and Mir, M.I. 2008. Recovery performance of partially fractured reservoirs by capillary imbibition. *J. Pet. Sci. Eng.* **60** (1): 39–50. doi: 10.1016/j.petrol.2007.05.008.

Hassanizadeh, S.M., Celia, M.A., and Dahle, H.K. 2002. Dynamic Effect in the Capillary Pressure—Saturation Relationship and its Impacts on Unsaturated Flow. *Vadose Zone J.* **1:** 38–57.

Kazemi, H., Gilman, J.R. and Elsharkawy, A.M. 1992. Analytical and Numerical Solution of Oil Recovery From Fractured Reservoirs With Empirical Transfer Functions. *SPE Res Eng* **7** (2): 219–227. SPE-19849-PA. doi: 10.2118/19849-PA.

Kazemi, H., Seth, M.S., and Thomas, G.W. 1969. The Interpretation of Interference Tests in Naturally Fractured Reservoirs with Uniform Fracture Distribution. *SPE J.* **9** (4): 463–472; *Trans.,* AIME, **246.** SPE-2156-PA. doi: 10.2118/2156-PA.

Lake, L.W. 1996. *Enhanced Oil Recovery*. Englewood Cliffs, New Jersey, USA: Prentice Hall.

Leverett, M.C. 1941. Capillary Behavior in Porous Solids. *Trans.,* AIME, **142:** 152–169.

Namdar Zanganeh, M., Salimi, H., and Bruining, J. 2007. Upscaling in Fractured Reservoirs Using Homogenization. Paper SPE 107383 presented at the EUROPEC/EAGE Conference and Exhibition, London, 11–14 June. doi: 10.2118/107383-MS.

Nelson, R.A. 1985. *Geologic Analysis of Naturally Fractured Reservoirs*, Vol. 1. Houston: Contributions in Petroleum Geology and Engineering, Gulf Publishing Company.

Rossen, W.R., Gu, Y., and Lake, L.W. 2000. Connectivity and Permeability in Fracture Networks Obeying Power-Law Statistics. Paper SPE 59720 presented at the SPE Permian Basin Oil and Gas Recovery Conference, Midland, Texas, USA, 21–23 March. doi: 10.2118/59720-MS.

Saidi, A.M. 1975. Mathematical simulation model describing Iranian fractured reservoirs and its application to Haft-Kel field. *Proc.,* World Petroleum Congress, Tokyo, 209–219.

Saidi, A.M. 1983. Simulation of Naturally Fractured Reservoirs. Paper SPE 12270 presented at the SPE Reservoir Simulation Symposium, San Francisco, 15–18 November. doi: 10.2118/12270-MS.

Sarma, P. and Aziz, K. 2006. New Transfer Functions For Simulations of Naturally Fractured Reservoirs with Dual-Porosity Models. *SPE J.* **11** (3): 328–340. SPE-90231-PA. doi: 10.2118/90231-PA.

Shook, M., Lake, L.W., and Li, D. 1992. Scaling immiscible flow through permeable media by inspectional analysis. *In Situ* **16** (4): 311–349.

Stearns, D.W. 1969. Fracture as a Mechanism of Flow in Naturally Deformed Layered Rocks. *Proc.,* Conference on Research in Tectonics (Kink Bands and Brittle Deformation), Ottawa, Canada, 14–15 March 1968, GSC Paper 68-52, 79–96.

Stearns, D.W. and Friedman, M. 1972. Reservoirs in Fractured Rock. In *AAPG Memoir 16, Stratigraphic Oil and Gas Fields—Classification, Exploration Methods, and Case Histories*, 82–100. Tulsa: AAPG.

van Duijn, C.J., Molenaar, J., and deNeef, M.J. 1995. The effect of capillary forces on immiscible two-phase flow in heterogeneous porous media. *Transport in Porous Media* **21** (1): 71–93. doi: 10.1007/BF00615335.

van Golf-Racht, T. 1982. F*undamentals of Fractured Reservoir Engineering*, Vol 12. Oxford, UK: Elsevier Publishing Company.

Warren, J.E. and Root, P.J. 1963. The Behavior of Naturally Fractured Reservoirs. *SPE J.* **3** (3): 245–255; *Trans.,* AIME, **228.** SPE-426-PA. doi: 10.2118/426-PA.

Wu, Y.-S., Liu, H.H., and Bodvarsson, G.S. 2004. A triple-continuum approach for modeling flow and transport processes in fractured rock. *J. of Contaminant Hydrology* **73** (1–4): 145–179. doi: 10.1016/j.jconhyd.2004.01.002.

Appendix A—Effective Fracture Permeability

Collecting the terms of order $1/\varepsilon$ in Eq. 4 leads to

$$\nabla_s \cdot k_f^* k_{r\alpha,f}^{(0)} \left[\nabla_b \Phi_{\alpha f}^{(0)} + \nabla_s \Phi_{\alpha f}^{(1)} \right] = 0 \quad \text{in } \Omega_f, \quad \ldots\ldots\ldots\ldots (A\text{-}1)$$

and collecting the terms of order $\varepsilon^{(0)}$ in Eq. 6, we obtain

$$k_f^* k_{r\alpha,f}^{(0)} \left[\nabla_b \Phi_{\alpha f}^{(0)} + \nabla_s \Phi_{\alpha f}^{(1)} \right] \cdot \mathbf{n} = 0 \quad \text{on } \partial\Omega_m. \quad \ldots\ldots\ldots\ldots (A\text{-}2)$$

In order to proceed we assume that $\Phi^{(1)}_{\alpha f} = \boldsymbol{\omega} \cdot \text{grad}_b \, \Phi^{(0)}_{\alpha f}$. Substitution of this into Eq. A-1 leads to:

$$\nabla_s \cdot \left[k_f^* k_{r\alpha,f}^{(0)} \left(\mathbf{I} + \nabla_s \otimes \boldsymbol{\omega} \right) \cdot \nabla_b \Phi_{\alpha f}^{(0)} \right] = 0 \quad \text{in } \Omega_f, \quad \ldots\ldots\ldots (A\text{-}3)$$

where we have used that $\nabla_s \Phi^{(0)}_{\alpha f} = 0$, and the boundary condition is as follows

$$\left[k_f^* k_{r\alpha,f}^{(0)} \left(\mathbf{I} + \nabla_s \otimes \boldsymbol{\omega} \right) \cdot \nabla_b \Phi_{\alpha f}^{(0)} \right] \cdot \mathbf{n} = 0 \text{ on } \partial\Omega_m. \quad \ldots\ldots\ldots (A\text{-}4)$$

On the scale of the unit cell, we may assume that $\nabla_b \Phi^{(0)}_{\alpha f}$ is a vector with constant components. Therefore, we may investigate the result when the unit cell is subjected to a unit potential gradient [i.e., $\nabla_b \Phi^{(0)}_{\alpha f} = -\mathbf{e}_x$]. In this case, Eq. A-3 reduces to

$$\nabla_s \cdot \left[k_f^* k_{r\alpha,f}^{(0)} \nabla_s \otimes \boldsymbol{\omega} \right] = 0 \quad \text{in} \quad \Omega_f, \quad \ldots\ldots\ldots\ldots\ldots (A\text{-}5)$$

and the BC

$$k_f^* k_{r\alpha,f}^{(0)} \left(\nabla_s \otimes \boldsymbol{\omega} \right) \cdot \mathbf{n} = -k_f^* k_{r\alpha,f}^{(0)} \mathbf{I} \cdot \mathbf{n} \quad \text{on} \quad \partial\Omega_m. \quad \ldots\ldots\ldots (A\text{-}6)$$

To obtain the average fracture permeability, we write the first right term of Eq. 9 after averaging

$$\begin{aligned}
&\frac{1}{|\Omega|} \int_{\Omega_f} \nabla_b \cdot \frac{k_f^* k_{r\alpha,f}^{(0)}}{\mu_{\alpha,f}} \left[\nabla_b \Phi_{\alpha f}^{(0)} + \nabla_s \Phi_{\alpha f}^{(1)} \right] d\mathbf{x}_s \\
&\quad = \frac{1}{|\Omega|} \int_{\Omega_f} \nabla_b \cdot \frac{k_f^* k_{r\alpha,f}^{(0)}}{\mu_{\alpha,f}} \left[\nabla_b \Phi_{\alpha f}^{(0)} + \nabla_b \Phi_{\alpha f}^{(0)} \nabla_s \otimes \omega \right] d\mathbf{x}_s \\
&\quad = \frac{1}{|\Omega|} \int_{\Omega_f} \nabla_b \cdot \frac{k_f^* k_{r\alpha,f}^{(0)}}{\mu_{\alpha,f}} \left(\mathbf{I} + \nabla_s \otimes \omega \right) \nabla_b \Phi_{\alpha f}^{(0)} d\mathbf{x}_s = . \quad \ldots\ldots (A\text{-}7) \\
&\quad = \frac{1}{|\Omega|} \int_{\Omega_f} \nabla_b \cdot \frac{k_{r\alpha,f}^{(0)}}{\mu_{\alpha,f}} k_f^* \left(\mathbf{I} + \nabla_s \otimes \omega \right) \nabla_b \Phi_{\alpha f}^{(0)} d\mathbf{x}_s = \\
&\quad = \nabla_b \cdot \frac{k_{r\alpha,f}^{(0)}}{\mu_{\alpha,f}} k_f \nabla_b \Phi_{\alpha f}^{(0)}
\end{aligned}$$

We define the average fracture permeability as follows:

$$k_f = \frac{1}{|\Omega|}\int_{\Omega_f} k_f^*\left(\mathbf{I}+\nabla_s \otimes \omega\right)\mathrm{d}\mathbf{x}_s. \quad \text{(A-8)}$$

Appendix B—Numerical Solution

The 0th-order terms of upscaled two-phase-flow equations based on homogenization of the fracture system are as follows:

$$\begin{cases} \phi_f \dfrac{\partial S_{\alpha f}^{(0)}}{\partial t} + \dfrac{\phi_m}{|\Omega|}\displaystyle\int_{\Omega_m} \dfrac{\partial S_{\alpha m}^{(0)}}{\partial t}\mathrm{d}x_s \\ -\nabla_b \cdot \left[k_f \dfrac{k_{r\alpha,f}^{(0)}}{\mu_{\alpha,f}}\nabla_b \Phi_{\alpha f}^{(0)}\right] = q_\alpha,\ \alpha = o,w, \\ \Phi_{\alpha f} = p_{\alpha f} + \rho_\alpha g z, \\ \Phi_{cf} = \Phi_{of} - \Phi_{wf} = p_{cf}\left(S_{wf}\right) \\ +\left(\rho_o - \rho_w\right) g z, \\ S_{wf} + S_{of} = 1 \end{cases}, \quad \text{(B-1)}$$

where ϕ_f and k_f are the effective (global) fracture porosity and the effective fracture permeability, respectively. The matrix equations are

$$\begin{cases} \phi_m \dfrac{\partial S_{\alpha m}^{(0)}}{\partial t} - \nabla_s \cdot \left[k_m \dfrac{k_{r\alpha,m}^{(0)}}{\mu_{\alpha,m}}\nabla_s \Phi_{\alpha m}^{(0)}\right] = 0,\ \alpha = o,w, \\ \Phi_{\alpha m} = p_{\alpha m} + \rho_\alpha g z, \\ \Phi_{cm} = \Phi_{om} - \Phi_{wm} = p_{cm}\left(S_{wm}\right) + \left(\rho_o - \rho_w\right) g z, \\ S_{wm} + S_{om} = 1, \\ \Phi_{\alpha m}\left(t, x_b, x_s\right) = \Phi_{\alpha f}\left(t, x_b\right) \quad \text{on } \partial M \end{cases}. \quad \text{(B-2)}$$

The systems B-1 and B-2 include six independent variables, two phase pressures, potentials, and saturations; we can reduce this number to two. Using the volume balance relation, we can eliminate one of the saturations; moreover, the capillary pressure relation allows us to eliminate one of the two pressures. Finally, the pressures are also functions of the potentials and can be eliminated. We are thus left only to discretize the nonlinear partial-differential equations:

$$\begin{cases} \phi_f \dfrac{\partial S_{wf}}{\partial t} + \dfrac{\phi_m}{|\Omega|}\displaystyle\int_{\Omega_m} \dfrac{\partial S_{wm}}{\partial t}\mathrm{d}x_s \\ -\nabla_b \cdot \left(k_f \dfrac{k_{rw,f}}{\mu_{w,f}}\nabla_b \Phi_{wf}\right) = q_w, \\ -\nabla_b \cdot \left(k_f \dfrac{k_{rw,f}}{\mu_{w,f}}\nabla_b \Phi_{wf}\right) \\ -\nabla_b \cdot \left[k_f \dfrac{k_{ro,f}}{\mu_{o,f}}\nabla_b \left(\Phi_{wf} + \Phi_{cf}\right)\right] = q_w + q_o \end{cases}, \quad \text{(B-3)}$$

$$\begin{cases} \phi_m \dfrac{\partial S_{wm}}{\partial t} - \nabla_s \cdot \left(k_m \dfrac{k_{rw,m}}{\mu_w}\nabla_s \Phi_{wm}\right) = 0, \\ -\nabla_s \cdot \left(k_m \dfrac{k_{rw,m}}{\mu_w}\nabla_s \Phi_{wm}\right) \\ -\nabla_s \cdot \left[k_m \dfrac{k_{ro,m}}{\mu_o}\nabla_s \left(\Phi_{wm} + \Phi_{cm}\right)\right] = 0, \\ \left.\begin{array}{l}\Phi_{wm}\left(t, x_s, x_b\right) = \Phi_{wf}\left(t, x_b\right), \\ \Phi_{cm}\left(S_{wm}\right) = \Phi_{cf}\left(S_{wf}\right),\end{array}\right\} \text{ on } \partial M \end{cases}. \quad \text{(B-4)}$$

A backward Euler time discretization is used on the systems B-3 and B-4. For time level t^n, we have partial-differential equations in $\mathbf{x}_s$ for each fixed $\mathbf{x}_b$ for the matrix water potential Φ^n_{wm} and matrix water saturation S^n_{wm}, with Φ^n_{wf} and S^n_{wf} as the two parameters of the system. We further discretize systems B-3 and B-4 in space by applying a finite-volume method. This reduces the system to a fully discrete, finite-dimensional problem. Let the number of fracture unknowns be I, and denote them at time level t^n by

$$\vec{\chi}_f^n = \left\{\Phi^n_{wf,i}, S^n_{wf,i}, i = 1,2,\ldots,I\right\}. \quad \text{(B-5)}$$

The numerical method requires only a matrix block at each gridpoint in the fracture system. Then associated with each gridpoint $i = 1, 2, \ldots, I$, there is a series of matrix unknowns

$$\vec{\chi}_{m,i}^n = \left\{\Phi^n_{wm,ij}, S^n_{wm,ij}, j = 1,2,\ldots,J_i\right\}, \quad \text{(B-6)}$$

in the ith matrix block. Let

$$\vec{\chi}_m^n = \left\{\Phi^n_{wm,ij}, S^n_{wm,ij}, i = 1,2,\ldots,I,\ j = 1,2,\ldots,J_i\right\}. \quad \text{(B-7)}$$

The fully discrete nonlinear equations then take the form

$$\begin{cases} F_i\left(\vec{\Phi}^n_{wf}, \vec{S}^n_{wf}, \vec{\Phi}^n_{wm}, \vec{S}^n_{wm}\right) = 0, & i = 1,2,\ldots,I, \\ M_{ij}\left(\Phi^n_{wf,i}, S^n_{wf,i}, \vec{\Phi}^n_{wm,i}, \vec{S}^n_{wm,i}\right) = 0, & i = 1,2,\ldots,I,\ j = 1,2,\ldots,J_i, \end{cases} \quad \text{(B-8)}$$

for some nonlinear functions F_i and M_{ij}.

One way to solve nonlinear equations of this form is to use Newton's method. Let $\vec{\Phi}^{n,m}_{wf}, \vec{S}^{n,m}_{wf}$, and $\vec{\Phi}^{n,m}_{wm}, \vec{S}^{n,m}_{wm}$, denote the mth Newton iterate for solution at the nth timestep, let D_π denote partial differentiation with respect to π, and let

$$F_i^{n,m-1} = F_i\left(\vec{\Phi}^{n,m-1}_{wf}, \vec{S}^{n,m-1}_{wf}, \vec{\Phi}^{n,m-1}_{wm}, \vec{S}^{n,m-1}_{wm}\right),$$
$$M_{ij}^{n,m-1} = M_{ij}\left(\Phi^{n,m-1}_{wf,i}, S^{n,m-1}_{wf,i}, \vec{\Phi}^{n,m-1}_{wm,i}, \vec{S}^{n,m-1}_{wm,i}\right).$$

Then, the Newton procedure can be described as the following iterative process:

1. Start with an initial guess for the solution

$$\vec{\Phi}^{n,0}_{wf}, \vec{S}^{n,0}_{wf}, \text{ and } \vec{\Phi}^{n,0}_{wm}, \vec{S}^{n,0}_{wm}.$$

2. For each $m = 1, 2, \ldots$, until convergence is reached:

(a) Solve for

$$\delta\vec{\phi}^{n,m}_{wf}, \delta\vec{S}^{n,m}_{wf}, \text{ and } \delta\vec{\phi}^{n,m}_{wm}, \delta\vec{S}^{n,m}_{wm},$$

satisfying

$$\begin{cases} F_i^{n,m-1} + \displaystyle\sum_{i'}\left[\begin{array}{l} D_{\phi_{wf,i'}} F_i^{n,m-1}\delta\phi^{n,m}_{wf,i'} + D_{S_{wf,i'}} F_i^{n,m-1}\delta S^{n,m}_{wf,i'} \\ +\displaystyle\sum_{j'}\left(\begin{array}{l} D_{\phi_{wm,i'j'}} F_i^{n,m-1}\delta\phi^{n,m}_{wm,i'j'} \\ +D_{S_{wm,i'j'}} F_i^{n,m-1}\delta S^{n,m}_{wm,i'j'} \end{array}\right) \end{array}\right] \\ = 0,\quad i = 1,2,\ldots,I, \\ M_{ij}^{n,m-1} + D_{\phi_{wf,i}} M_{ij}^{n,m-1}\delta\phi^{n,m}_{wf,i} + D_{S_{wf,i}} M_{ij}^{n,m-1}\delta S^{n,m}_{wf,i} \\ +\displaystyle\sum_{j'}\left(\begin{array}{l} D_{\phi_{wm,ij'}} M_{ij}^{n,m-1}\delta\phi^{n,m}_{wm,ij'} \\ +D_{S_{wm,ij'}} M_{ij}^{n,m-1}\delta S^{n,m}_{wm,ij'} \end{array}\right) = 0, i = 1,2,\ldots,I,\ j = 1,2,\ldots,J_i; \end{cases} \quad \text{(B-9)}$$

(b) Define

$$\vec{\phi}^{n,m}_{wf} = \vec{\phi}^{n,m-1}_{wf} + \delta\vec{\phi}^{n,m}_{wf},\quad \vec{S}^{n,m}_{wf} = \vec{S}^{n,m-1}_{wf} + \delta\vec{S}^{n,m}_{wf},$$
$$\vec{\phi}^{n,m}_{wm} = \vec{\phi}^{n,m-1}_{wm} + \delta\vec{\phi}^{n,m}_{wm},\quad \vec{S}^{n,m}_{wm} = \vec{S}^{n,m-1}_{wm} + \delta\vec{S}^{n,m}_{wm}.$$

Within the linearized Newton problem, the matrix solution in the ith block is an affine operator of $\Phi^{n,m}_{wf,i}$ and $S^{n,m}_{wf,i}$. Therefore, one can decouple the matrix and fracture problems without affecting the implicit nature of the scheme. The matrix problem in Eq. B-9 is replaced by the following three problems for

$$\left(\tilde{\delta}\vec{\phi}^{n,m}_{wm},\tilde{\delta}\vec{S}^{n,m}_{wm}\right),\ \left(\hat{\delta}\vec{\phi}^{n,m}_{wm},\hat{\delta}\vec{S}^{n,m}_{wm}\right),\ \text{and}\ \left(\bar{\delta}\vec{\phi}^{n,m}_{wm},\bar{\delta}\vec{S}^{n,m}_{wm}\right).$$

For each $i = 1, 2, \ldots, I$ and $j = 1, 2, \ldots, J_i$,

$$\begin{cases} D_{\phi_{wf,i}} M^{n,m-1}_{ij} + \sum_{j'} \begin{pmatrix} D_{\phi_{wm,ij'}} M^{n,m-1}_{ij} \tilde{\delta}\phi^{n,m}_{wm,ij'} \\ +D_{S_{wm,ij'}} M^{n,m-1}_{ij} \tilde{\delta}S^{n,m}_{wm,ij'} \end{pmatrix} = 0, \\ D_{S_{wf,i}} M^{n,m-1}_{ij} + \sum_{j'} \begin{pmatrix} D_{\phi_{wm,ij'}} M^{n,m-1}_{ij} \hat{\delta}\phi^{n,m}_{wm,ij'} \\ +D_{S_{wm,ij'}} M^{n,m-1}_{ij} \hat{\delta}S^{n,m}_{wm,ij'} \end{pmatrix} = 0, \\ M^{n,m-1}_{ij} + \sum_{j'} \begin{pmatrix} D_{\phi_{wm,ij'}} M^{n,m-1}_{ij} \bar{\delta}\phi^{n,m}_{wm,ij'} \\ +D_{S_{wm,ij'}} M^{n,m-1}_{ij} \bar{\delta}S^{n,m}_{wm,ij'} \end{pmatrix} = 0 \end{cases} \quad \ldots\ldots\text{(B-10)}$$

The result is that

$$\begin{aligned} \delta\phi^{n,m}_{wm,ij} &= \tilde{\delta}\phi^{n,m}_{wm,ij}\delta\phi^{n,m}_{wf,i} + \hat{\delta}\phi^{n,m}_{wm,ij}\delta S^{n,m}_{wf,i} + \bar{\delta}\phi^{n,m}_{wm,ij}, \\ \delta S^{n,m}_{wm,ij} &= \tilde{\delta}S^{n,m}_{wm,ij}\delta\phi^{n,m}_{wf,i} + \hat{\delta}S^{n,m}_{wm,ij}\delta S^{n,m}_{wf,i} + \bar{\delta}S^{n,m}_{wm,ij} \end{aligned} \quad \ldots\ldots\ldots\text{(B-11)}$$

We thus modify Step 2a of the Newton algorithm by first solving the system of Eq. B-10. The fracture δ-potential and fracture δ-saturation are then given by solving the fracture equations of B-9, using implicitly the definition of Eq. B-11. Finally, we explicitly use the fracture δ-potential and δ-saturation and Eq. B-11 to update the matrix δ-potential and δ-saturation.

Hamidreza Salimi is a PhD student of reservoir engineering in the department of geotechnology at Delft U. of Technology. His current research includes upscaling in fractured reservoirs to improve the prediction of oil recovery, studying imbibition processes using a glass micromodel, and developing a mathematical model for closing thief zones in carbonate oil reservoirs by using acids. Salimi is the recipient of the 2008 SPE Nico van Wingen Memorial Graduate Fellowship in Petroleum Engineering. He holds an MSc degree in chemical and petroleum engineering from Sharif U. of Technology in Tehran, Iran. **Hans Bruining** is professor of geo-environmental engineering at Delft U. of Technology. He holds MSc and PhD degrees in physical chemistry from the U. of Amsterdam. Bruining's current research concerns upscaled models of fractured reservoirs, modeling and experiments of thermal recovery, greenhouse gas (CO_2) application and sequestration related to fossil fuel recovery, underground coal gasification, and applications of EOR techniques for remediation of polluted soils.